

New mitigation methods for transient overvoltages in gas insulated substations

Simon Burow

Universität Stuttgart
simon.burow@ieh.uni-stuttgart.de
Germany

Uwe Riechert

ABB Switzerland Ltd
uwe.rieichert@ch.abb.com
Switzerland

Wolfgang Köhler

Universität Stuttgart
wolfgang.koehler@ieh.uni-stuttgart.de
Germany

Stefan Tenbohlen

Universität Stuttgart
stefan.tenbohlen@ieh.uni-stuttgart.de
Germany

ABSTRACT

During switching of disconnectors (DS) in GIS a varying number of pre-strikes and re-strikes occur. Due to the very short duration of the voltage collapse, traveling surges are generated in the busbar duct. These very fast transient overvoltages (VFTO) can become the limiting dielectric stress which defines the dimensions at UHV voltage levels. The decision shall be based on the maximum VFTO peak value that occurs with reference to the rated lightning impulse withstand voltage (LIWV) of the equipment. If the maximum VFTO is higher than the LIWV, it is necessary to consider the VFTO level as dimensioning criteria or to suppress VFTO by suitable measures.

The main challenges are the reduction in VFTO amplitudes and finally the reduction of the effects of VFTO on the equipment. For the different sources of VFTO and for the different equipment different mitigation methods are known. The damping of VFTO by integration of a damping resistor is a well proven technology. The way to overcome the drawback of such unwieldy designs is to use other internal damping measures. Several methods have been proposed and examined in the past, such as ferrite material or high frequency (RF) resonators.

The VFTO damping solution utilizing ferrite rings has been analysed and tested and will be described here. The measurements show that a damping effect can be achieved, but with an important drawback: the magnetic material goes easily into saturation, which complicates the design and reduces its general applicability and robustness.

A new approach for damping is to implement compact electromagnetic high-frequency resonators with low quality factor specially designed to cover a wider frequency range. The novelty of this idea is not only to design the resonators but also to dissipate the VFTO energy. The VFTO damping effect of the developed RF resonator tuned to the dominant harmonic component was confirmed by experiments.

Rings of a nanocrystalline alloy placed around the GIS conductor were also investigated. Depending on number, material and size of the rings a good mitigation could be achieved.

1 INTRODUCTION

During switching of disconnectors in GIS a varying number of pre-strikes and re-strikes occur. Due to the very short duration of the voltage collapse, traveling waves are generated in the busbar duct. The multiple refractions and reflections of these waves at impedance discontinuities within the enclosures create complex waveforms, which depend on the DS design, the operating conditions and the configurations of the GIS. The transients are characterized by their short duration and very high frequencies. The rise times are in the range of some ns, with dominant frequency components up to 100 MHz. The VFTO can become the limiting dielectric stress which defines the dimensions at UHV voltage levels [4]. The first three switchgear installations in the UHV demonstration project in China are partially executed using gas-insulated design or as hybrid systems (Hybrid-IS), that is, as a combination of air-insulated and gas-insulated components. One of these installations is being supplied by ABB/Xi'an Shiky as Hybrid-IS shown in Figure 1. Based on test and simulation results it was decided that no VFTO mitigation measures are required for the Hybrid-IS design [5].



Figure 1: Pictures of 'Jingmen' 1100 kV substation

2 VERY FAST TRANSIENT OVERVOLTAGES (VFTO)

2.1 Rise time and Peak Value

The maximum amplitude of the VFTO depends on the voltage drop at the DS just before striking and the location considered. A trapped charge on the load side resulting in a voltage of -1 pu (per unit) is normally used for the calculation of VFTO as the most unfavorable case for high speed DS or phase opposition conditions [2]. For this case the maximum VFTO peak in GIS configuration has a typical value between 1.5 pu and 2.8 pu. Extremely high values of more than 3.0 pu have been reported. It can be shown, however, that these values have been derived by calculation using unrealistic simplified simulation models [1]. VFTO in GIS are of greater concern at the highest rated voltages, for which the ratio of the LIWV to the system voltage is lower [2]. The maximum calculated VFTO in GIS system may reach the insulation level of LIWV.

The generation and propagation of VFTO from their original location throughout a GIS can produce internal and external transient overvoltages (see Figure 2). The main concerns are internal overvoltages between the conductor and the enclosure. Internal VFTO cause high stress of the insulation system [7]. External VFTO can be dangerous for secondary and adjacent equipment. These external transients include transient voltages between the enclosure and ground at GIS-air interfaces, voltages across insulating spacers in the vicinity of GIS current transformers, when they do not have a metallic screen on the outside surface, voltages on the secondary terminals of instrument transformers, radiated electromagnetic fields (EMF) which can be dangerous to adjacent control or relay equipment [7].

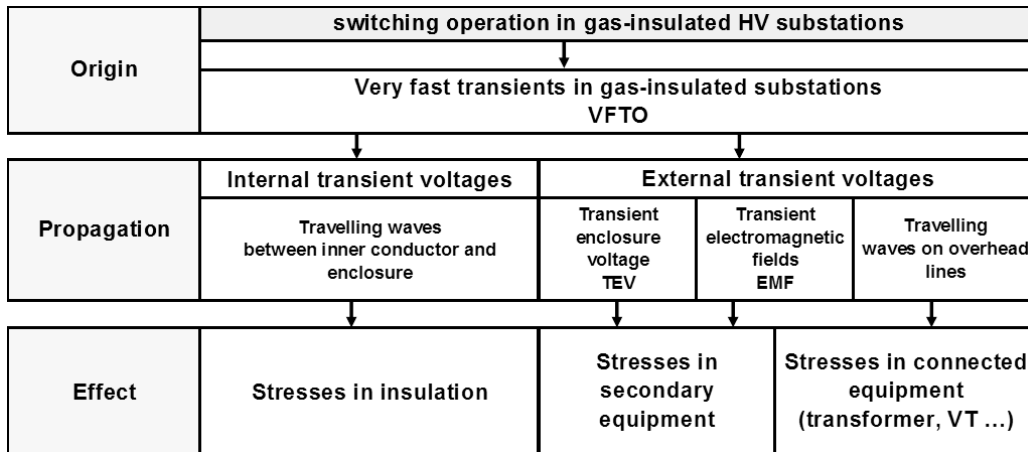


Figure 2: Classification of VFTO in high voltage GIS substation

For the discussion about the severity of the traveling waves, a detailed analysis of the current/voltage characteristics is necessary. The voltage collapse during the spark development provides the excitation function for the transients. After the formation time lag has passed, an additional phase with the duration t_b (spark formation time) is needed to complete the breakdown, which is followed by the voltage collapse. The spark formation time itself is given by the *Toepler's* spark law. Due to the high breakdown field of SF₆ and the higher gas pressure nanosecond rise times can be estimated in GIS. Measurements in a 550 kV and 1100 kV gas-insulated DS showed rise times between 3 ns and 10 ns depending on the gas pressure and field utilization factor at the time of the strike (see Figure 3). The rise times of overvoltages generated by an air-insulated DS are in the range between 0.4 μs and 1.5 μs, as shown in Figure 3 [8]. Beside the lower rise time, traveling waves on overhead lines are also characterized by lower frequency components.

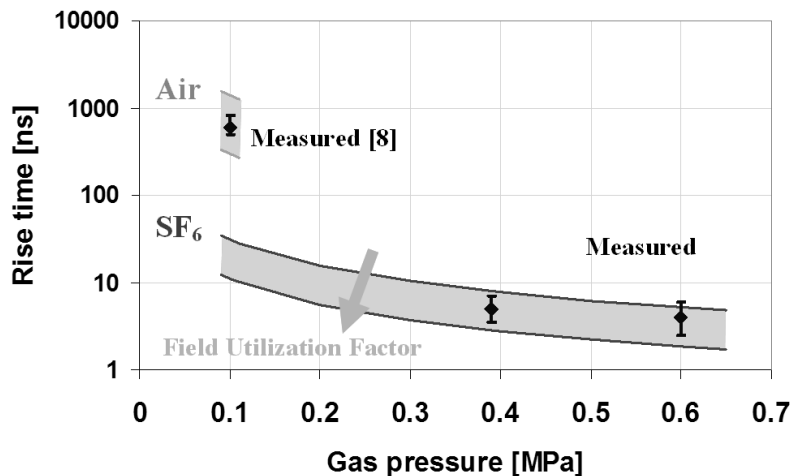


Figure 3: Spark formation time for SF₆ and air (calculated and measured values)

2.2 Influence of substation layout

The propagation of VFTO throughout GIS can be analyzed by representing GIS sections as low-loss distributed parameter transmission lines. Each section may be characterized by the surge impedance and the time of travelling. Travelling waves are reflected and refracted at every point where they encounter a change in the wave impedance. The generated transients depend on the GIS configuration and on the superposition of the surges reflected and refracted on line discontinuities like circuit-breakers, T-junctions, cable connections or bushings. Thereby, the main frequencies depend on the length of the GIS sections. Due to the travelling wave behavior of the VFTO, the overvoltages show a spatial distribution. Normally, the highest overvoltage stress is reached at the open end of the load side. For the calculation of VFTO stresses, the trapped charge remaining on the load side of the DS must be taken into consideration. For the first simulations a value of -1 pu (worst case) was used.

Figure 4 (left – case A) shows a very simple case: a GIS busbar. The reflections of the travelling wave at both terminals produce at the open end a pulse-shaped transient of constant magnitude of +3 pu and constant frequency (Figure 5 - left). Maximum voltages can reach higher values in more complex GIS configurations. Figure 4 (right – case B) shows a T-junction GIS network. The simulations show that the voltage at the open end of the longer busbar section is higher. The worst case occurs if the length ratio between the two busbars is in the range of 2 (for comparison see Figure 6). The fact that each GIS contains T- or X-connections gives an indication, that the maximum VFTO in GIS is normally higher compared to a Hybrid-IS.



Figure 4: Model network; left: case A, right: case B

Figure 5 (right) shows the simulation result obtained with a more realistic representation of the source ($R = 10 \Omega$). The frequency is still the same. The maximum VFTO at the open end is lower for both cases and the transient is damped. The maximum voltage for case B is 3.3 pu.

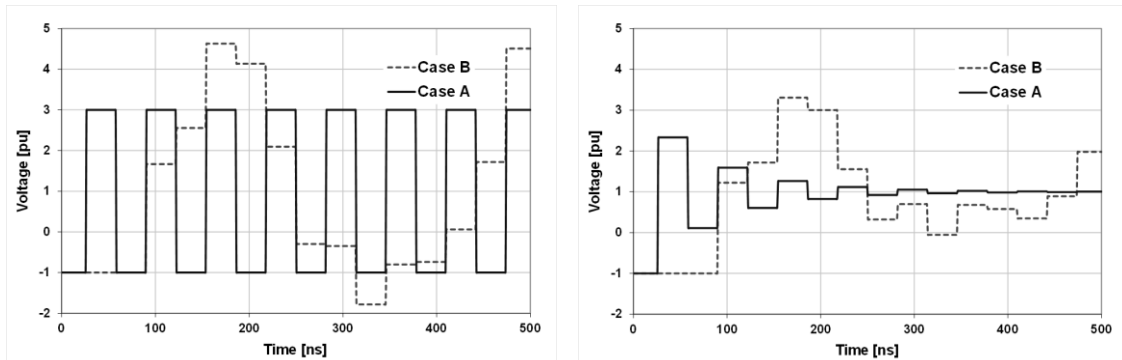


Figure 5: Simulation results with trapped charge voltage of -1 pu; left: ideal source, right: $R = 10 \Omega$

Depending on the design of the disconnector (especially contact speed, dielectric design of the contacts and SF_6 gas pressure) the assumption of trapped charge resulting in -1 pu voltage is a very conservative assumption for VFTO calculations [5]. For a slow acting DS ($< 1 \text{ m/s}$) the trapped charges were evaluated statistically [4]. The evaluation of type test results for the 1100 kV DS have revealed that the 99 % voltage associated with trapped charges where 0.45 pu at a source voltage of 1 pu. Figure 6 shows that the voltage at the open end for case B is reduced to a value of 2.7 pu (-20 %) by using a realistic value for the trapped charge voltage [3].

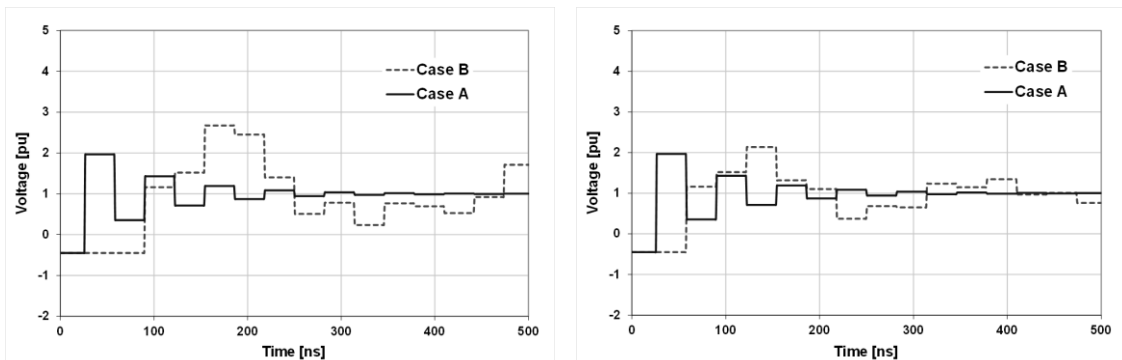


Figure 6: Simulation results with trapped charge voltage of -0.45 pu; right: the length of both busbars in case B was set to 10 m

It can be concluded, that in most cases the maximum VFTO is lower in Hybrid-IS compared to a GIS. Based on a literature survey, it can be assumed, that the maximum VFTO peak value in GIS using the

worst case assumption for the trapped charge voltage of -1 pu is lower than 2.5 pu to 2.6 pu [2]. Whereas for a Hybrid-IS, the maximum reported value is lower than 2.2 pu. Using a realistic value for the trapped charge voltage of -0.45 pu the maximum VFTO value is lower than 2.1 pu for GIS or 1.8 pu for Hybrid-IS. Because the generated transients depend strongly on the specific configuration and on the superposition of travelling waves it is not possible to give generally admitted values, valid for each case. An accurate simulation for each substation, especially in the UHV range, is necessary for the insulation co-ordination as basis for the decision making about possible countermeasures. The accuracy of VFTO simulations itself depends strongly on the quality of the model of each individual component. Therefore, it is important to verify the simulation results by measurements [3].

2.3 Other VFTO sources

VFTO appearing in GIS are caused not only by DS operation. Other events, such as the operation of a circuit-breaker, the occurrence of a line-to-ground fault or the closing of an earthing switch can also cause VFTO [2]. However, during a DS operation a high number of re-strikes and pre-strikes occur due to the low operating speed of DS compared to a circuit-breaker.

A flashover or breakdown within GIS produces VFTO. If the breakdown occurs in an almost homogeneous field, a maximum voltage enhancement factor of 1.7 compared to the applied voltage peak has to be assumed. In case of a breakdown at a defect the voltage collapse time is longer and this leads to a higher damping and a lower enhancement factor of 1.45 [6]. Nevertheless, subsequent breakdowns at defects with inhomogeneous field distribution may result. Therefore the breakdown to earth is of special concern during on-site testing.

Because of the trapped charge voltage remaining on the busbar, a making operation of an earthing switch can produce VFTO. The maximum VFTO measured during the field test of the 1100 kV GIS in Japan was 1.13 pu.

Circuit-breaker may also generate transients in GIS. But due to their very fast operation only a few number of strikes occur. VFTO occur during making of CB. Especially under out-of-phase conditions, the amplitude can reach values up to 2 pu. A larger number of re-strikes may occur for the special case of switching of small inductive current during shunt-reactor switching.

2.4 VFTO mitigation

For the different sources of VFTO and for the different equipment many mitigation methods are known. The damping of VFTO by integration of a damping resistor is a well proven technology [2]. The resistance of the damping resistor could be chosen and defined according to the maximum calculated VFTO and the required mitigation effect. The VFTO decreases with increasing resistance; and the dimension of the disconnecter increases with increasing resistance. In addition special requirements regarding the rate of rise of the voltage across the resistor, the energy absorption and the branching behaviour must be taken into account. A flashover across the resistor may lead to very high amplitude VFTO compared to a DS without such a damping resistor, and thus must be avoided. The way to overcome the drawback of such unwieldy designs is to use other internal damping measures.

3 EXPERIMENTAL SETUP

The high voltage test setup consists mainly of a 550 kV GIS from ABB type ELK-3. A schematic diagram is shown in Figure 7. The VFTOs in the GIS are generated by a breakdown between the spark gap. For this purpose a standard high voltage impulse generator injects a surge voltage via a bushing inside the GIS. The spark gap consists of two spherical electrodes and is situated in SF₆ atmosphere. As the surge voltage reaches the breakdown voltage of the spark gap, a sparkover occurs between the contacts and initiates the VFTOs.

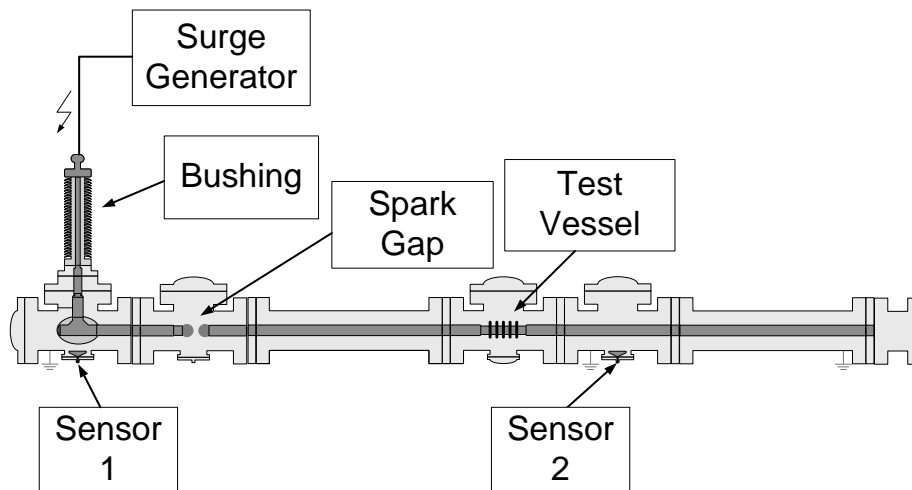


Figure 7: Schematic diagram of the high voltage test setup: GIS with spark gap, capacitive voltage sensors and a flexible test vessel for different test installations

By means of the SF₆ pressure and the distance of the spark gap, it is possible to control the breakdown voltage of the spark gap and thereby the amplitude of VFTOs as well. There are two possibilities to terminate the GIS at the end. If the end of the inner conductor is not grounded, it forms an open termination and the transient voltage waves are reflected by a positive factor close to +1. Elsewise the inner conductor is connected with two copper strips at the end to the enclosure. The transient voltage waves are reflected by a negative factor close to -1. In a test vessel with one additional flange and flexible inner conductor different testing objects (e.g. ferrite rings and resonator) could easily be installed. On both sides of the test vessel capacitive voltage sensors are installed in a flange of the GIS enclosure, enabling very accurate measurement. The testing arrangement is presented in Figure 8.



Figure 8: The high voltage test setup in the laboratory of University of Stuttgart: ABB 550 kV GIS type ELK-3 with bushing

This setup enables to generate VFTOs with an amplitude up to 800 kV and more. The dominant harmonic component of the VFTO frequency spectrum is approximately 15 MHz for the GIS setup without ground strips and about 7.5 MHz for the GIS setup with a short-circuited termination. It is related to the reflection at the ends and the total length of the GIS.

For a precise measurement of VFTOs two special developed capacitive voltage sensors were mounted inside the GIS. The sensors consist mainly of a double layer board and are shown in Figure 9. The layer facing to the grounded GIS enclosure is connected to the enclosure by the flange and a copper RF-seal directly. The top layer forms a capacitance to both the grounded layer and the inner conductor of the GIS (stray capacitance). This high frequency capacitive voltage divider has a divider ratio of some 10 000. The top layer is connected to a BNC-connector.

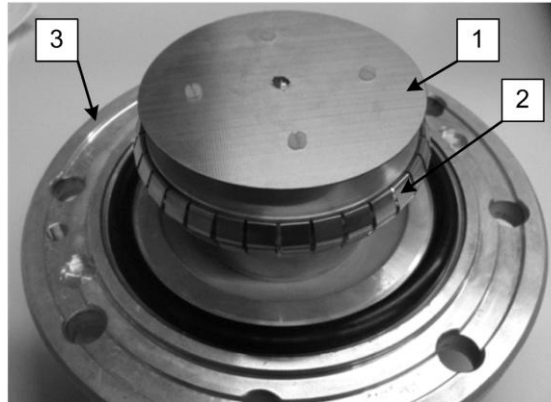


Figure 9: The capacitive sensor which was made at the University of Stuttgart: It consists mainly of a double layer board (1) which forms a capacitive voltage divider. The board and a copper RF-seal (2) are mounted on a flange cover plate (3)

The signals of the sensors are recorded by an oscilloscope (LeCroy waveRunner 104 MXi, used Bandwidth: 200 MHz). Before analysing the results, always 10 signals were superimposed to avoid impacts caused by small variation of the breakdown voltage.

4 VFTO MITTIGATION METHODS

4.1 Ferrite material for VFTO damping

The VFTO damping solution utilizing ferrite rings has been proposed and investigated in the literature e.g. in [8]. Mostly the ferrite rings were tested under low voltage conditions or simulations were carried out. In this chapter the results of high voltage tests with different ferrite rings and ferrite arrangements will be discussed. Therefore the rings were placed around the inner conductor inside the GIS. For the tests the GIS setup with short-circuited end was used.

Rings of different ferrite materials were investigated and the number of rings inside the GIS was varied between 1 and 6. Also the diameter of the rings was different. The rings are shown in Figure 10.

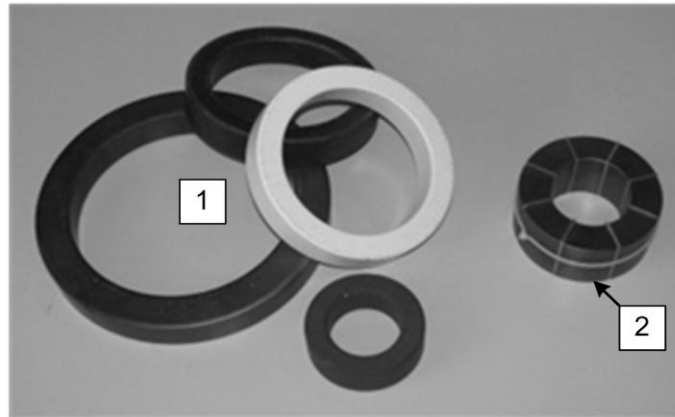


Figure 10: Different kind of ferrite rings (1) and a sheared ferrite ring arrangement with gaps of epoxy resin (2)

Figure 11 shows as an example the VFTO measurement result with and without 6 ferrite rings. The mitigation effects in a full-scale HV arrangement are negligible.

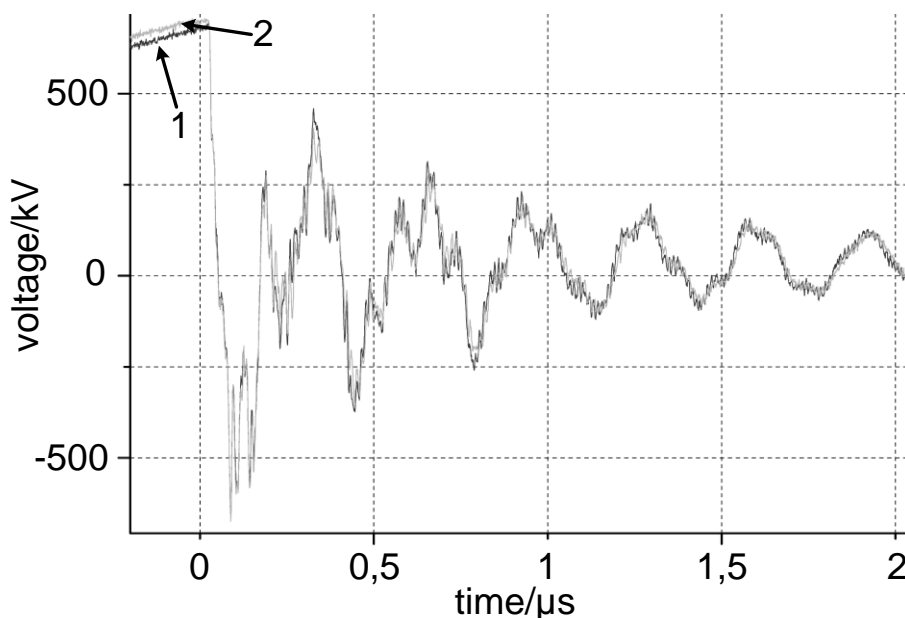


Figure 11: Comparison of VFTOs with a maximum amplitude of about 700 kV and a dominant harmonic component of approximately 7.5 MHz: Line 1 represent VFTOs without rings. VFTOs with 6 ferrite rings are shown in line 2.

In comparison to previous studies the current through the rings is much higher but represents the situation in real GIS. The impedance of the GIS setup is approximately 70Ω . Therefore VFTOs with an amplitude of 700 kV lead to a current of about 10 kA. Therefore, the intensity of the magnetic field around the conductor is also very high. This high magnetic field saturates the ferrite material completely. As a consequence the damping effect is reduced to a marginal value.

By layering of ferrite rings it is possible to increase the magnetic field strength at which the material saturates. On the other hand layering of rings with a material of lower permeability also reduces the effective permeability. Therefore, the damping efficiency of the whole ring arrangement decreases. Figure 10 shows a layered arrangement of ferrite segments with plates of epoxy resin as known from conductor boards. Tests with this ring arrangement however show no VFTO mitigation effect.

Based on the test results it could be concluded that the damping effect of ferrite rings inside the GIS for HV applications is limited. The reason is the high current of VFTOs which causes a completely saturation of the ferrite material. Saturated ferrite materials lose their damping capability.

4.2 High frequency RF resonator for VFTO damping

A new approach for mitigation of VFTOs is to implement a compact electromagnetic RF resonator with optimised quality factor (Q). The resonator could be installed inside the GIS and gets stimulated by the VFTOs. For example, a cavity of an electric shielding could serve as a resonator. The novelty of this idea is not only the design of the low Q resonator. Also the dissipating of the VFTO energy must be investigated.

RF resonators for damping of VFTOs in GIS should have a special geometrical shape to avoid a negative effect on the dielectric behaviour of the GIS. From the dielectric design viewpoint, a suitable shape of the resonator should be elongated along the axis of the inner conductor in order to achieve a suitable resonant frequency with a minimum size in the radial direction. In addition to this the outer surface of the resonator should be smooth (rounded) in order to avoid electric field enhancement regions such as sharp edges and corners.

Figure 12 shows a resonator schematically as it is used for first simulations and tests. The resonator consists of an aluminium tube which is connected to the inner conductor on one side. The other side of the tube forms a thin, but long gap between resonator and inner conductor.

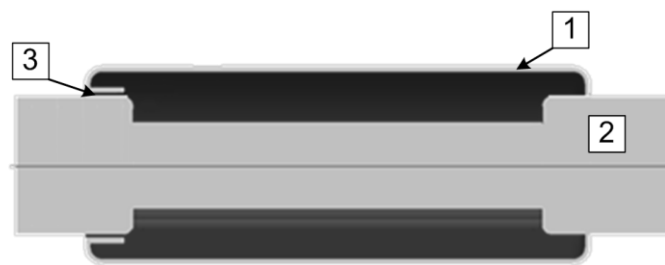


Figure 12: Schematic drawing of a resonator: An aluminium tube (1) is arranged around the inner conductor of the GIS (2). A long and thin gap (3) between resonator and conductor is formed on one side of the tube.

Since the magnetic field of the resonator is distributed over the cavity volume, the cavity size will determine the resonator magnetic inductance L. The gap between resonator and inner conductor forms the space of an electric field enhancement. Therefore the electric capacitance C of the resonator is determined by this gap. Having the resonator inductance L and capacitance C, it is possible to compute its resonant frequency f using equation [1].

$$f = \frac{1}{2\pi\sqrt{LC}} \quad [1]$$

f	Resonance frequency
L	Inductance
C	Capacitance

It is not always straightforward to compute analytically the inductance and capacitance of each resonator geometry. A general solution of this problem is the so-called eigenvalue analysis (resonance search) of a resonator based on full-Maxwell electromagnetic field simulations that is presently a common approach for the design of microwave resonators [10], [11]. In this approach, the source-free Maxwell equations are discretized by using the finite element method (FEM). This process results in a large sparse homogenous system of linear equations. The mathematical eigenvalues of this system correspond to the resonant frequencies of the resonator and could be analysed performing time-domain and frequency-domain eigenvalue analysis [10].

The simulations verify a significant damping of VFTOs. The optimum damping could be achieved by termination of the gap with a resistor which equals the characteristic impedance of the resonator. Also the resonant frequency of the resonator has to be in the range of the dominant harmonic component of the VFTO. In this case a significant part of the energy of the VFTO is stored in the resonator. By dissipating the energy of the resonator a mitigation of VFTO will be achieved.

In order to verify the results experimentally, two test arrangements were designed. The length of the first resonator is below 1 m and it has a resonant frequency of about 57 MHz which is much higher compared to the dominant harmonic frequency component of the GIS setup. As a consequence the resonant frequency of the resonator has to be reduced.

As the gap between resonator and inner conductor forms the capacitance C and the cavity of the resonator represents the inductance L , an increase of one or both of these parameters decreases the resonant frequency of the resonator. For the tests the resonant frequency was adjusted by means of additional external capacitors in the gap.

If the adjusted resonator gets stimulated by the VFTOs sparking occurs in the gap. For the chosen resonator design the spark resistance have not been sufficient to mitigate the VFTOs. To increase the mitigation effect an additional resistor was mounted in the gap. The connected resistor is not homogeneous distributed around the gap and therefore not an ideal termination. But using this simple solution, a slight damping effect was achieved as shown in Figure 13.

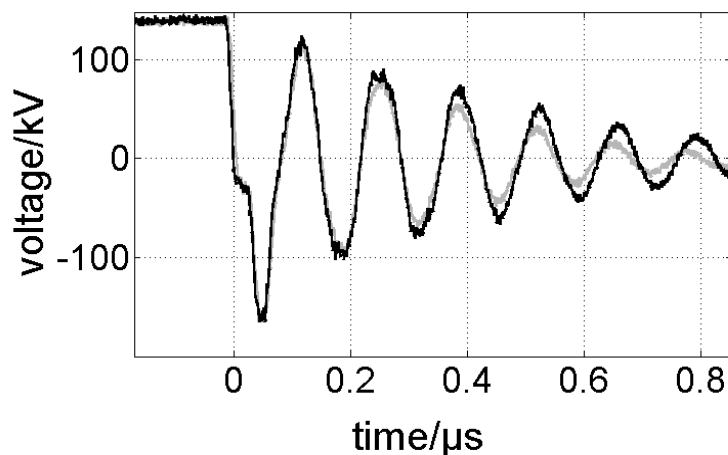


Figure 13: Comparison of VFTOs in a GIS with a resistor fitted resonator (grey line) vs. a GIS without a resonator (black line)

Since the parameters of the resonator could be changed in a wide range, this resonator design could be optimized in the future in order to increase its damping efficiency. Further investigation and tests will be performed with this setup using a new optimized resonator.

4.3 Nanocrystalline material for VFTO damping

Very promising results were found by using rings of a nanocrystalline alloy. To obtain VFTO mitigation these rings are arranged around the inner conductor of the GIS like the ferrite rings (Figure 14 right). Experiments with different ring types, different sizes and different numbers of rings were carried out.

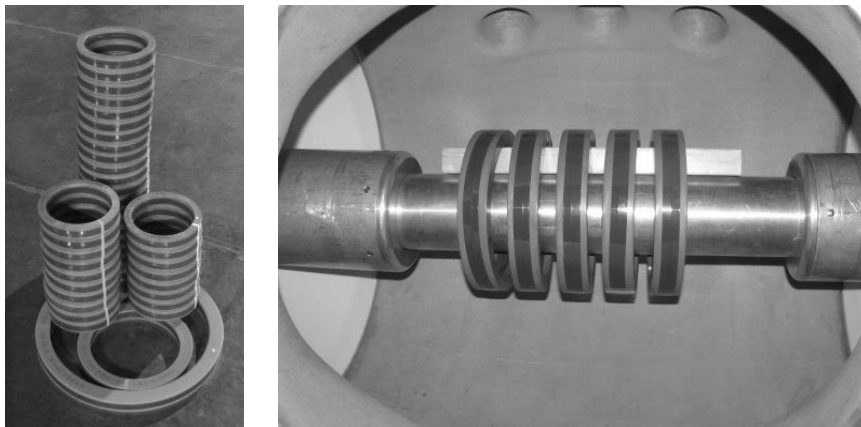


Figure 14: Nanocrystalline rings with different permeability and diameters (left). Five rings mounted inside the GIS for VFTO tests (right).

The used alloy is based on iron (Fe) with silizium (Si), boron (B) and other additives [12]. By means of a rapid solidification technology the liquid metal is converted to very thin ribbons with a thickness of approximately 20 μm . The thin tape is wound up to rings. Finally a heat treatment with temperatures between 500 and 600 $^{\circ}\text{C}$ transforms the initially amorphous microstructure of the tape into the desired nanocrystalline state with fine crystalline grains embedded in an amorphous residual phase. The average grain diameter is between 10 and 40 nm. This material has very specific properties which could be adjusted by means of an external magnetic field during the heat treatment. Especially the permeability and the saturation flux density of these rings are very high.

Different rings with an external diameter between 20 cm and 50 cm and a permeability between 8 000 and 45 000 were used (Figure 14 left). The rings were installed inside the GIS setup as shown in Figure 14. Surge voltage, SF_6 pressure and gap distance were kept constant for all tests to ensure equal conditions. Figure 15 exemplifies the difference between VFTOs measured during a test without rings and with 20 rings inside the GIS. It is obviously that the VFTOs are damped by the rings. Even the amplitude of the first peaks was significantly reduced by 20 %.

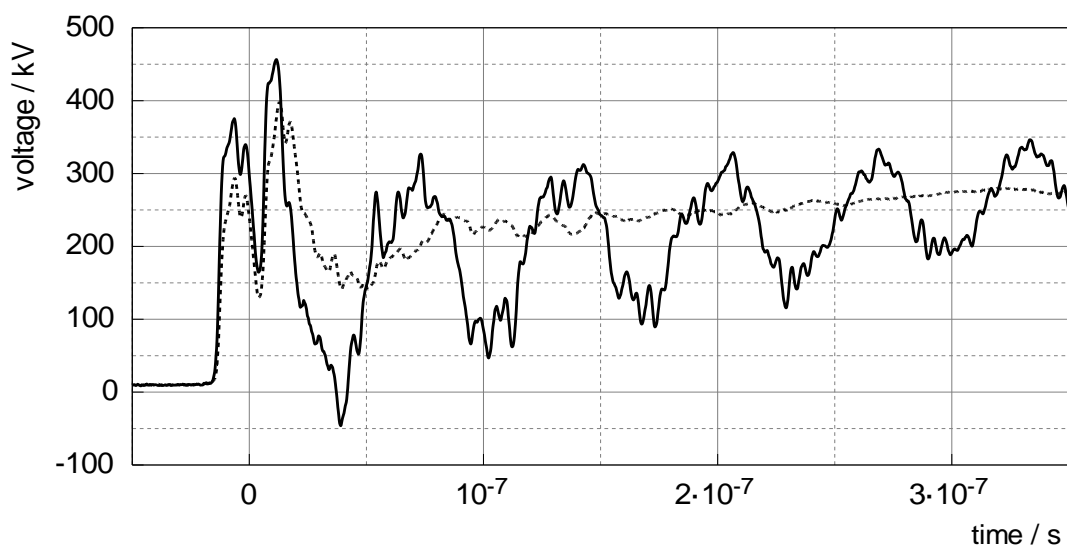


Figure 15: VFTOs without rings (continuous line) and with 20 rings (dashed line) measured on sensor 2.

Further investigation with different rings and numbers leads to following qualitative conclusions:

- More rings increases the damping effect. This relationship seems to be approximately linear.
- A higher permeability increases the damping effect.

The tested rings with an outer diameter of 50 cm consist of a wider tape than the rings with a diameter of 20 cm. So the total material volume of the larger rings is much higher. On the other hand the magnetic field decreases by $1/r$. Finally, the damping effect of rings with different sizes but same permeability was approximately the same.

A further challenge is a suitable place for the rings to avoid local dielectric overstress. It is not appropriate to place the rings at any place around the inner conductor as it was done during the tests. A possible solution is presented in Figure 16. The rings are placed under a metallic shielding. Tests with this arrangement have shown the same mitigation effect.

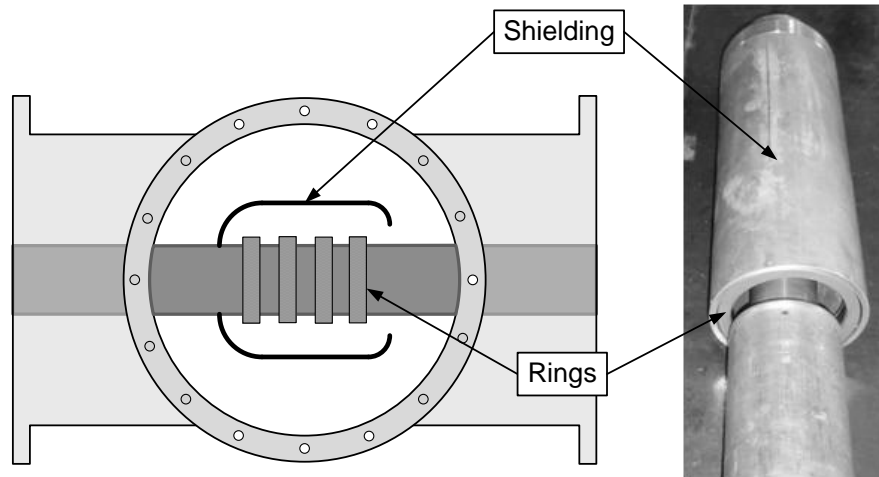


Figure 16: Schematic drawing (left) and test setup (right) of a shielding for the nanocrystalline rings

5 SUMMARY

Before starting the design of an UHV substation, it has to be clarified whether VFTO have significant influence on the insulation co-ordination. The decision shall be based on the maximum VFTO peak value that occurs with reference to the rated lightning impulse withstand voltage of the equipment. If the maximum VFTO is below the LIWV, no measures need to be taken. Otherwise it is necessary to design considering the VFTO level as dimensioning criteria or to suppress VFTO by damping devices. For the different sources of VFTO and for the different equipment different mitigation methods are known. The damping of VFTO by integration of a damping resistor is one proven technology. The way to overcome the drawback of such unwieldy design is to use other internal damping measures such as ferrite materials or RF resonators. The VFTO damping solution utilizing ferrite rings has been analysed and tested. The measurements show that the damping effect can be achieved, but with an important drawback: the magnetic material goes easily into saturation, which complicates the design and reduces its general applicability and robustness.

A new approach for damping is to implement compact electromagnetic high-frequency resonators with low quality factor specially designed to cover a wider frequency range. The novelty of this idea is not only in designing the resonators but also in dissipating the received VFTO energy. The VFTO damping effect of the developed RF resonator tuned to the dominant harmonic component was confirmed by experiments.

Rings of a nanocrystalline alloy placed around the GIS conductor leads also to a significant mitigation effect. Depending on number, material and size of the rings good results could be achieved.

LITERATUR

- [1] CIGRÉ Brochure 362 Working Group A3.22: “*Technical Requirements for Substations Equipment Exceeding 800 kV - Field experience and technical specifications of Substation equipment up to 1200 kV*”, December 2008
- [2] CIGRÉ Brochure 456 Working Group A3.22: “*Background of Technical Specifications for Substation Equipment Exceeding 800 kV AC*”, April 2011
- [3] Riechert, U.; Neumann, C.; Hama, H.; Okabe, S.; Schichler, U., on behalf of CIGRÉ WG D1.36 and AG D1.03: “*Basic Information and Possible Counter Measures Concerning Very Fast Transients in Gas-Insulated UHV Substations as Basis for the Insulation Co-ordination*”, CIGRÉ SC A2 & D1 Joint Colloquium 2011, Kyoto, Japan, PS3-O-5
- [4] Riechert, U.; Krüsi, U.; Sologuren-Sanchez, D.: “*Very Fast Transient Overvoltages during Switching of Bus-Charging Currents by 1100 kV Disconnecter*”, CIGRÉ Report A3-107, 43rd CIGRÉ Session, August 22-27, 2010, Palais des Congrès, Paris, France
- [5] Riechert, U.; Holaus, W.: “*Ultra High Voltage Gas-Insulated Switchgear – A Technology Milestone*”, Euro. Trans. Electr. Power (2011), (wileyonlinelibrary.com). DOI: 10.1002/etep.582
- [6] CIGRÉ Working Group 15.03: “*GIS Insulation Properties in Case of VFT and DC Stress*”, Report 15-201, 36th CIGRÉ Session, Aug. 25-31, 1996, Paris, France
- [7] CIGRÉ Working Group 33/13-09: “*Monograph on GIS Very Fast Transients*”, Brochure 35, July 1989
- [8] Del Pozo, M.D.; Esteban, D.A.; Issouribehere, P.E.; Barbera, G.A.; Funes, A.; Ledesema, A.: “*Field measurements and modelling of high frequency transients during disconnect switch operations in EHV Substations. Assessment of their effects on Current Transformers*”, CIGRÉ Report A3-207, 43rd CIGRÉ Session, August 22-27, 2010, Palais des Congrès, Paris, France
- [9] J. Lijun, Z. Yicheng, Z. Xiangong, S. Yuzhuo, “*Characteristic parameter analysis on the suppressing VFTO in GIS by ferrite*”, Proceedings of 2005 International Symposium on Electrical Insulating Materials, Vol. 3, pp. 825 – 828, 2005
- [10] Smajic, J.; Holaus, W.; Troeger, A.; Burow, S.; Brandl, R.; Tenbohlen, S.: “*HF Resonators for Damping of VFTs in GIS*”, Proceedings of the 9th Int. Conference on Power System Transients (IPST2011), Paper ID:185, Delft University of Technology, The Netherlands, June 2011
- [11] Smajic, J.; Holaus, W.; Kostovic, J.; Riechert, U.: “*3D Full-Maxwell Simulations of Very Fast Transients in GIS*”, IEEE Transactions on Magnetics, Vol. 47, No. 5, pp. 1154-1517, May 2011
- [12] MAGNETEC GmbH: <http://www.magnetec.de/>, product information “*Cool Blue*®”, Germany, January 2012